

# Surface Potential Dependence of the Hamaker Constant

Hang Li,<sup>\*,†</sup> Xuhong Peng,<sup>‡</sup> Laosheng Wu,<sup>§</sup> Mingyun Jia,<sup>†</sup> and Hualin Zhu<sup>†</sup>

College of Resources and Environment, Southwest University, Chongqing, 400716, P. R. China, Instrument Analysis and Research Center, Lanzhou University, 730000, Lanzhou, P. R. China, and Department of Environment Sciences, University of California, Riverside, California 92521

Received: September 21, 2008; Revised Manuscript Received: January 15, 2009

Hamaker constant is a key parameter in the study of particle interactions of materials. Even though there are quite a few methods for measuring the Hamaker constant, the current experimental results showed that the obtained Hamaker constants from different methods for the same material usually had considerable variations. In this paper, a new method for determination of the Hamaker constant was suggested: the Hamaker constant can be easily measured through determination of the swelling pressure of the material in aqueous solution. In this paper, the Hamaker constants of 36 different montmorillonites with different surface potentials were obtained by the method. The results showed that the Hamaker constant of montmorillonite was surface potential dependent. At values of the surface potential larger than  $-267$  mV, the values of the Hamaker constant increased with an increase of the surface potential; nevertheless, at surface potentials lower than  $-267$  mV, the Hamaker constant appeared to decrease with an increase of the surface potential.

## 1. Introduction

Nanoparticles or colloidal particles interactions are an important issue in a wide range of scientific and technological fields. The DLVO theory has been demonstrated to be a theory that can give a quantitative description for nanoparticles or colloidal particles interaction,<sup>1</sup> even though for some special cases the non-DLVO forces may have importance.<sup>1</sup> In the DLVO theory, two forces were considered: the electric repulsive force between two adjacent particles due to the overlap of the electric double layer (EDL) of counterions and the long-range van der Waals attractive force. In recent research, non-DLVO forces, e.g., hydration force, etc., have been detected for charged colloidal particles in aqueous suspensions.<sup>2–8</sup> However, this force exists only for two surfaces of particles closer than  $1.5$  nm.<sup>3,6,8</sup> In the application of the DLVO theory, a key and difficult issue is how to obtain the Hamaker constant.

There are quite a few methods for measuring the Hamaker constant, including the dielectric constant determination method,<sup>9,10</sup> surface force apparatus method (SFA)<sup>11,12</sup> and recently atomic force microscope method (AFM).<sup>13–17</sup> Unfortunately, the different methods for same material showed the obtained Hamaker constants to be considerable variations.<sup>18</sup>

The Hamaker constant is usually treated as a material property, but recent research has shown that it might not always be the case. Wensink and Jérôme<sup>19</sup> and Kaya<sup>20</sup> found it might be density dependent. Castellanos et al. found that the Hamaker constant was temperature dependent.<sup>21</sup>

In this paper, we discuss a new method for determination of the Hamaker constant through measurement of the swelling pressures of materials in aqueous solution and found that the Hamaker constant is surface potential dependent. The experi-

mental data for the swelling pressure were cited from the experiments performed by Low for 36 different montmorillonites in aqueous solution.<sup>22</sup> The reasons we use those experimental data are as follows. (1) Low simultaneously determined the surface charges, surface area, and water content under different applied pressures of the montmorillonites, making it so the van der Waals force and the electric repulsive force can be estimated simultaneously. (2) The difference among those 36 different montmorillonites is just the surface charge number (or surface potential under given conditions), which came from the difference of isomorphic substitution for different montmorillonites. Therefore, the 36 different montmorillonites provided ideal materials to estimate the influence of the surface potential on the van der Waals force. (3) With the amount of experimental data reaching 36, this ensures the reliability of the obtained results.

## 2. New Approach for Hamaker Constant Determination

According to the DLVO theory, the van der Waals force makes particles attract together and the electric repulsive force of EDL makes particles repel each other. As the repulsive force is stronger than the attractive force, the particles will disperse in the medium and form a suspension. For this case, only as we exert an external pressure on the system, will the particles become closer to an extent; the stronger the external pressure is, the closer the particles will be. Suppose the applied external pressure is  $P_{\text{ext}}$  (atm), which equals the net swelling pressure at equilibrium. Therefore, assuming the corresponding average distance between two adjacent particles surfaces is  $\lambda$  (dm) at this applied pressure we have

$$P_{\text{ext}}(\lambda) = P_{\text{EDL}}(\lambda) - P_{\text{vdw}}(\lambda) \quad (1)$$

where  $P_{\text{EDL}}$  is the pressure (atm) from the electric repulsive force and  $P_{\text{vdw}}$  is the pressure (atm) from the van der Waals force.

\* To whom correspondence should be addressed. Phone: 086-023-68250674. E-mail: hli22002@yahoo.com.cn.

<sup>†</sup> Southwest University.

<sup>‡</sup> Lanzhou University.

<sup>§</sup> University of California, Riverside.

TABLE 1: Surface and Zeta Potentials of 36 Different Montmorillonites (mV)

montmorillonite	zeta potential	surface potential	montmorillonite	zeta potential	surface potential
Aberdeen	-54.3	-269	Alaska	-53.0	-273
Argentine	-48.0	-269	Arizona	-48.0	-289
Belle Fourche	-55.6	-268	Blue Western	-46.7	-266
Chiguagua	-50.5	-281	Cameron	-65.7	-297
High grade Western	-49.3	-267	California Red Top	-65.7	-265
Czechoslovakian#1	-59.4	-265	Czechoslovakian#650	-54.3	-275
Danish	-59.4	-278	Guam	-55.6	-262
California	-51.8	-267	India	-49.3	-281
Italian	-54.3	-282	Louisiana	-53.1	-257
Mexican	-59.4	-286	Missouri	-55.6	-272
Monte Amiata	-60.6	-271	Nevada	-68.2	-284
New Mexico	-51.8	-286	New Zealand	-73.2	-289
Otay	-56.9	-293	Rio Escondido	-53.1	-274
Polkville	-50.5	-280	Romanian	-51.8	-268
Sardinian	-50.5	-283	Smithvill	-55.6	-267
Texas	-55.6	-279	Yellow Western	-64.4	-261
Upton	-67.0	-267	Western CA	-50.5	-274

Equation 1 is applicable only when the hydration force can be neglected, which comes from the interaction between the water molecule and the particle surface. However, the hydration force was observed at a distance shorter than 15 Å between surfaces of two particles.<sup>3,6,8</sup> Therefore, eq 1 is applicable when the distance between surfaces of two particles is larger than 15 Å.

The  $P_{EDL}$  can be calculated with the Langmuir equation; for 1:1 type electrolyte, it can be written as

$$P_{EDL}(\lambda) = \frac{2}{101} RT c_0 \left\{ \cosh \left[ \frac{F\phi(\lambda/2)}{RT} \right] - 1 \right\} \quad (2)$$

where  $\phi(\lambda/2)$  is the potential at the overlapping position of two DDLs ( $\lambda/2$ ) for two adjacent particles (units of V),  $c_0$  is the concentration of the electrolyte in bulk solution (units of mol/L),  $R$  is the gas constant (units of J/mol·K),  $T$  is the absolute temperature (units of K), and  $F$  is Faraday's constant (units of C). The units for  $P_{EDL}(\lambda)$  are atm in eq 2.

Therefore, for any given  $P_{ext}(\lambda)$ , if the corresponding  $\lambda$  can be determined, from eq 2, the  $P_{EDL}(\lambda)$  may be calculated. Then we introduce  $P_{ext}(\lambda)$  and  $P_{EDL}(\lambda)$  into eq 1;  $P_{vdw}(\lambda)$  can be calculated. Further introducing the obtained  $P_{vdw}(\lambda)$  into the following equation, eq 3, the effective Hamaker constant in the medium (water) can be obtained

$$P_{vdw}(\lambda) = \frac{A_{eff}}{0.6\pi} (10\lambda)^{-3} \quad (3)$$

where  $A_{eff}$  is the effective Hamaker constant (units of J). The units of  $\lambda$  are dm, and the units of  $P_{vdw}$  are atm here.

The Hamaker constant was defined in vacuum; therefore, the Hamaker constant of montmorillonite in vacuum is<sup>23</sup>

$$A = \left[ (A_{eff})^{\frac{1}{2}} + (A_{water})^{\frac{1}{2}} \right]^2 \quad (4)$$

where  $A_{water}$  is the Hamaker constant of water in a vacuum.

The above discussion shows that if  $P_{ext}$  is experimentally determined, the key in determining the Hamaker constant is how to obtain the values of  $\phi(\lambda/2)$ . Li et al. obtained an equation to calculate the value of  $\phi(\lambda/2)$  from the value of the surface potential  $\phi(0)$ ,<sup>24</sup> and later a more accurate equation was also

obtained for calculating  $\phi(\lambda/2)$ ; for 1:1 type of electrolyte, it can be expressed as<sup>25</sup>

$$\frac{1}{2} \left[ 1 + \left( \frac{1}{2} \right)^2 e^{\frac{2F\phi(\lambda/2)}{RT}} + \left( \frac{3}{8} \right)^2 e^{\frac{4F\phi(\lambda/2)}{RT}} \right] - \arcsine \frac{F\phi(0) - F\phi(\lambda/2)_d}{2RT} = \frac{1}{4} \lambda \kappa e^{-\frac{F\phi(\lambda/2)}{2RT}} \quad (5)$$

where  $\kappa$  is the Debye–Huckel parameter (units of 1/dm) and

$$\kappa = \sqrt{\frac{8\pi F^2 c_0}{\epsilon RT}}$$

where  $c_0$  is the concentration of the 1:1 type electrolyte in bulk solution (units of mol/L) and  $\epsilon$  is the dielectric constant; here it equals  $8.9 \times 10^{-10} \text{ C}^2/\text{J} \cdot \text{dm}$  for water.

Much research has shown that the zeta potential may be far below the surface potential.<sup>24,26,27</sup> Thus, even though Low determined the zeta potential of the montmorillonites, we will not use them as the surrogate of the surface potential. Since charges on the montmorillonite surface can be taken as a permanent charge, the following classic Gouy–Chapman equation (for 1:1 type of electrolyte) can be adopted to calculate the surface potential of the montmorillonites through the determined values of the surface charge density

$$\sigma_0 = -\frac{CEC}{S} = \sqrt{\frac{2\epsilon c_0 RT}{\pi}} \sinh \left[ \frac{F\phi(0)}{2RT} \right] \quad (6)$$

where  $\sigma_0$  is the surface charge density,  $CEC$  is the cation exchange capacity of montmorillonite, and  $S$  is the specific surface area of montmorillonite. As the distance between the water molecule and the charged particle surface is less than 5 Å, modification of the dielectric constant must be considered.<sup>28</sup> Therefore, if we use the dielectric constant of bulk water to calculate the electric repulsive force, the distance between two surfaces of the adjacent particles should be larger than 10 Å.

Since the values of  $CEC$  and  $S$  also have been determined by Low for montmorillonites,<sup>22</sup> introducing those values into eq 6, the corresponding surface potentials can be calculated. On introducing the value of the surface potential into eq 5,  $\phi(\lambda/2)$  can be obtained.

### 3. Results and Discussions

**3.1. Surface Potentials of Different Montmorillonites.** Both the surface potentials of the montmorillonites obtained from eq 6 and the zeta potentials determined by Low are shown in Table 1. The electrolyte is NaCl with a concentration of  $10^{-4}$  mol/L in bulk solution, and the temperature is  $T = 298$  K. From Table 1, it is clearly shown that the surface potential is much higher than the zeta potential.

**3.2. Estimation of the Average Distance between Two Adjacent Plates Surfaces of Montmorillonites ( $\lambda$ ) at Different Values of Applied Pressure ( $P_{\text{ext}}$ ).** The determined value of the mass ratio of water to montmorillonites ( $m_w/m_m$ ) under any given applied pressure consists of two contributions: the mass ratio of the interlayer or intracrystalline water to montmorillonite ( $m_w/m_m$ )<sub>intra</sub> and the mass ratio of intercrystalline water to montmorillonite ( $m_w/m_m$ )<sub>inter</sub>, there is<sup>22</sup>

$$m_w/m_m = (m_w/m_m)_{\text{inter}} + (m_w/m_m)_{\text{intra}} \quad (7)$$

For a given material,  $(m_w/m_m)_{\text{inter}}$  would be a constant, which would be independent from both the applied pressure and the specific surface area. However,  $(m_w/m_m)_{\text{intra}}$  would change with both the applied pressure and the specific surface area. Actually, under a given applied pressure,  $(m_w/m_m)_{\text{intra}}$  would be proportional to the specific surface area.<sup>22</sup> Therefore, eq 7 can be rewritten as

$$m_w/m_m = bS + (m_w/m_m)_{\text{inter}} \quad (8)$$

where  $b$  is a constant.

Equation 8 indicates that the plot of  $m_w/m_m$  vs  $S$  at any applied pressure will be a linear, and the intercept of the line will be the value of  $(m_w/m_m)_{\text{inter}}$ . The plots of  $m_w/m_m$  vs  $S$  at different applied pressures are shown in Figure 1. Figure 1 clearly shows that the experimental data of  $m_w/m_m$  vs  $S$  are in good agreement with the linear relationship at each applied pressure. On the other hand, since  $(m_w/m_m)_{\text{inter}}$  would be independent from pressure, the intercept of each line would be the same theoretically at different pressures. Figure 1 shows that for applied pressures of 7, 5, 4, and 3 atm, the intercepts are 0.3205, 0.3344, 0.3567, and 0.3207, respectively, which are approximately equal to each other, and the average of the intercepts is 0.333. However, for lower applied pressures (2 and 1 atm), the intercepts are far below this average value. This may be explained by the fact that, at lower applied pressure, since the total water content is high, the intercrystalline water only accounts for a relatively small portion of the total water amount; therefore, the experimental error for detecting the intercrystalline water becomes great at a low applied pressure. Thus, it is reasonable if we take  $(m_w/m_m)_{\text{inter}} = 0.333$ . Those discussions also imply that we could not directly use the slope of the linear equation, eq 8, to calculate the values of  $\lambda$ .

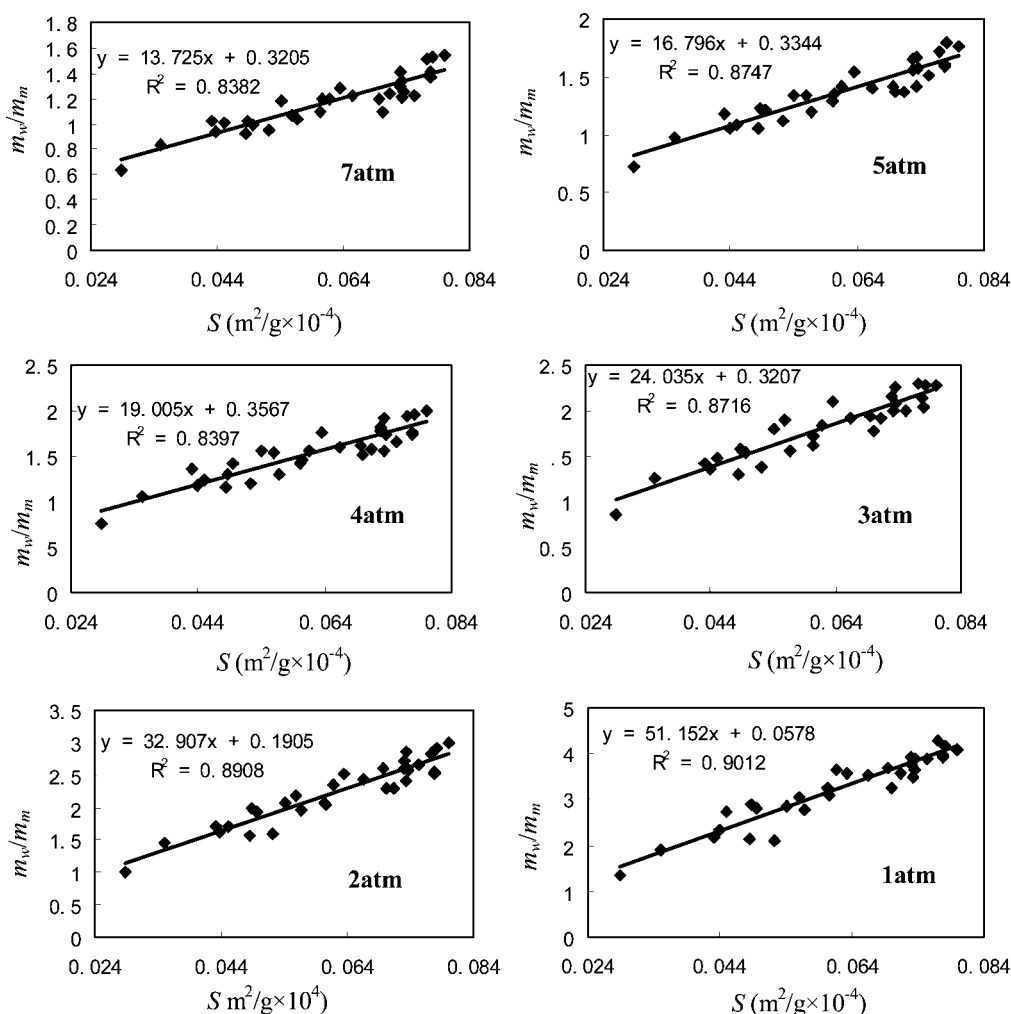


Figure 1. Experimental results of  $m_w/m_m$  vs  $S$  at different applied pressures.

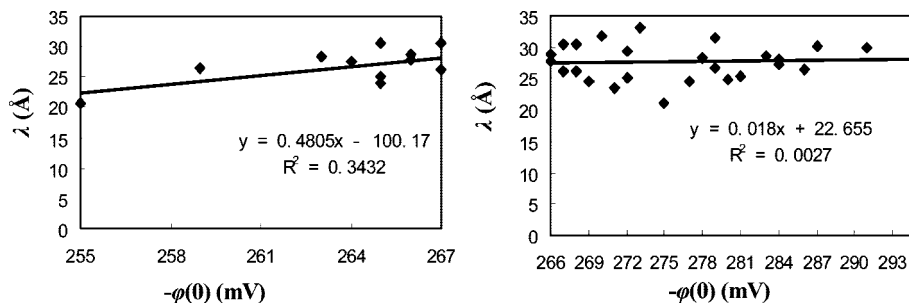


Figure 2. Relationship between  $\lambda$  and  $\varphi(0)$  at an applied pressure of 7 atm.

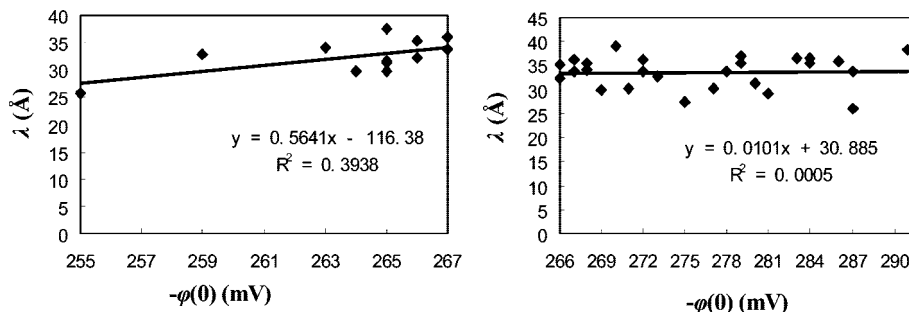


Figure 3. Relationship between  $\lambda$  and  $\varphi(0)$  at an applied pressure of 5 atm.

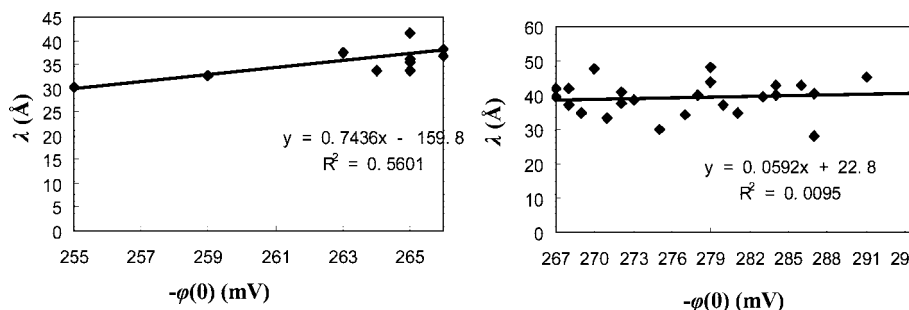


Figure 4. Relationship between  $\lambda$  and  $\varphi(0)$  at an applied pressure of 4 atm.

Because there is<sup>22</sup>

$$(m_w/m_m)_{\text{intra}} = 0.5\lambda S \quad (9)$$

introducing eq 9 into eq 7 and considering  $(m_w/m_m)_{\text{inter}} = 0.333$ , we get

$$\lambda = \frac{2}{S}(m_w/m_m - 0.333) \quad (10)$$

Using eq 10, the distance between two adjacent surfaces,  $\lambda$ , can be calculated at different applied pressures for each montmorillonite.

Considering the van der Waals force may be too weak as  $\lambda$  is large, in the following, we focus our discussion on the experimental results with applied pressures of 4, 5, and 7 atm. On the basis of eq 10, the obtained values of  $\lambda$  for montmorillonites with different surface potentials under given applied pressures of 4, 5, and 7 atm are shown in Figures 2, 3, and 4, respectively. The figures consistently show that at surface potentials below  $-267$  mV, at any given applied pressure, the values of  $\lambda$  increase with an increase of surface potential. However, at surface potentials of montmorillonites above  $-267$  mV, at any given applied pressure, the values of  $\lambda$  almost remain constant as the surface potential increases. According to the

TABLE 2: Values of  $\phi(\lambda/2)$  and  $P_{\text{vdw}}$  with Different Surface Potentials at an Applied Pressure of 7 atm

$\phi(0)$ , mV	$\lambda$ Å	$\phi(\lambda/2)$ , mV	$P_{\text{vdw}}$ , atm	$\phi(0)$ , mV	$\lambda$ Å	$\phi(\lambda/2)$ , mV	$P_{\text{vdw}}$ , atm
-255	22.49	-210.4	1.865	-275	27.61	-206.9	0.7349
-259	24.40	-208.5	1.232	-277	27.65	-207.2	0.8259
-263	26.20	-206.7	0.6749	-278	27.67	-207.3	0.8564
-264	26.67	-206.2	0.5268	-279	27.69	-207.5	0.9178
-265	27.20	-205.6	0.3528	-280	27.71	-207.6	0.9488
-266	27.45	-205.5	0.3242	-281	27.72	-207.8	1.011
-267	27.47	-205.6	0.3528	-283	27.76	-208.0	1.074
-268	27.49	-205.8	0.4104	-284	27.78	-208.1	1.105
-269	27.51	-206.0	0.4683	-286	27.81	-208.4	1.200
-270	27.52	-206.1	0.4975	-287	27.83	-208.5	1.232
-271	27.54	-206.3	0.5562	-291	27.90	-208.9	1.360
-272	27.56	-206.5	0.6153	-295	27.97	-209.3	1.493
-273	27.58	-206.6	0.645				

DLVO theory, as the surface potential is relatively higher, for a given material, the electric repulsive force between two plate surfaces will be stronger; as a result, for a given applied external pressure, the values of  $\lambda$  will increase with an increase of the surface potential. Therefore, the former case can be explained. The later case may be explained only as the van der Waals attractive force also increases as the surface potential increases for a given material.

**3.3. Estimation of  $P_{\text{vdw}}$  and  $\phi(\lambda/2)$  for Montmorillonites at Different Applied Pressures.** At different applied pressures, the values of  $\lambda$  have been obtained for different montmorillonites



**TABLE 3: Values of  $\phi(\lambda/2)$  and  $P_{\text{vdw}}$  with Different Surface Potentials at an Applied Pressure of 5 atm**

$\phi(0)$ , mV	$\lambda$ Å	$\phi(\lambda/2)$ , mV	$P_{\text{vdw}}$ , atm	$\phi(0)$ , mV	$\lambda$ Å	$\phi(\lambda/2)$ , mV	$P_{\text{vdw}}$ , atm
-255	27.51	-202.9	1.618	-275	33.66	-198.4	0.5538
-259	29.70	-200.8	1.098	-277	33.68	-198.6	0.5973
-263	32.00	-198.5	0.5755	-278	33.69	-198.8	0.6411
-264	32.52	-198.1	0.4892	-279	33.70	-198.9	0.6631
-265	33.13	-197.4	0.3623	-280	33.71	-199.0	0.6852
-266	33.58	-197.1	0.2794	-281	33.72	-199.1	0.7074
-267	33.58	-197.2	0.3000	-283	33.74	-199.4	0.7745
-268	33.59	-197.4	0.3415	-284	33.75	-199.5	0.7971
-269	33.60	-197.5	0.3624	-286	33.77	-199.7	0.8425
-270	33.61	-197.7	0.4043	-287	33.78	-199.8	0.8653
-271	33.62	-197.8	0.4254	-291	33.82	-200.2	0.9574
-272	33.63	-198.0	0.4679	-295	33.87	-200.6	1.051
-273	33.64	-198.1	0.4892				

**TABLE 4: Values of  $\phi(\lambda/2)$  and  $P_{\text{vdw}}$  with Different Surface Potentials at an Applied Pressure of 4 atm**

$\phi(0)$ , mV	$\lambda$ Å	$\phi(\lambda/2)$ , mV	$P_{\text{vdw}}$ , atm	$\phi(0)$ , mV	$\lambda$ Å	$\phi(\lambda/2)$ , mV	$P_{\text{vdw}}$ , atm
-255	30.10	-199.4	1.774	-275	39.08	-191.8	0.2939
-259	32.61	-197.0	1.259	-277	39.20	-191.9	0.3107
-263	35.58	-194.1	0.6967	-278	39.26	-191.9	0.3107
-264	36.30	-193.4	0.5703	-279	39.32	-192.0	0.3276
-265	37.11	-192.6	0.4300	-280	39.38	-192.0	0.3276
-266	38.00	-191.7	0.2772	-281	39.44	-192.1	0.3445
-267	38.69	-191.1	0.1783	-283	39.55	-192.2	0.3614
-268	38.69	-191.3	0.2110	-284	39.61	-192.2	0.3614
-269	38.72	-191.4	0.2275	-286	39.73	-192.3	0.3785
-270	38.78	-191.4	0.2275	-287	39.79	-192.3	0.3785
-271	38.84	-191.5	0.2440	-291	40.03	-192.5	0.4127
-272	38.90	-191.6	0.2605	-295	40.26	-192.6	0.4300
-273	38.96	-191.7	0.2772				

with different surface potentials in the above section. Because each  $\lambda$  is much larger than 15 Å, the hydration force and modification of the dielectric constant are not needed. As we introduce the values of  $\lambda$  and the corresponding values of  $\phi(0)$  into eq 5, the values of  $\phi(\lambda/2)$  can be calculated. Further introducing  $\phi(\lambda/2)$  into eq 2, the electric repulsive force  $P_{\text{EDL}}$  can be obtained. Finally, from eq 1, the van der Waals force can be calculated at any given applied pressure. The results are shown in Tables 2, 3, and 4 for different applied pressures of 7, 5, and 4 atm, respectively. The results clearly show that the van der Waals force is a function of the surface potential, and the patterns of the relationship between  $P_{\text{vdw}}$  and  $\phi(0)$  are the same for different applied pressures.

**3.4. Estimation of the Hamaker Constant for Different Montmorillonites.** Introducing the corresponding values shown in Tables 2, 3, and 4 into eq 3,  $A_{\text{eff}}$  can be calculated, and the obtained values of  $A_{\text{eff}}$  are shown in Table 5. Considering the Hamaker constant of water is  $A_{\text{water}} = 3.7 \times 10^{-20}$  J,<sup>10</sup> introducing the effective Hamaker constants listed in Table 5 into eq 4, the values of  $A$  can be obtained for different montmorillonites with different surface potentials; the results are shown in Figure 5.

Figure 5 clearly shows that the Hamaker constant is surface potential dependent for montmorillonites, and as the surface potential is lower than 267 mV in absolute value, the Hamaker constant decreases with increasing surface potential; nevertheless, at surface potentials higher than 267 mV in absolute value, the Hamaker constant increases with increasing surface potential. A question rises here, why does the Hamaker constant emerge from such a relationship with the surface potential of montmorillonite? We know that for a given colloidal suspension the

higher the surface potential is, the stronger the field strength will be. The electric field strength on the particle surface can be calculated from the following equation

$$E_0 = \sqrt{\frac{32\pi\epsilon_0 RT}{\epsilon}} \sinh\left[\frac{F\phi(0)}{2RT}\right] \quad (11)$$

For the montmorillonite/aqueous system with  $10^{-4}$  mol/L NaCl, as the surface potential increase from -255 to -295 mV, the electric field strength will increase from  $-1.21 \times 10^6$  to  $-2.80 \times 10^6$  V/cm. Therefore, we can consider that the montmorillonite “molecules” are located in a strong electric field with field strength higher than  $10^6$  V/cm in absolute value. With different strength of electric field, both the dipole moment and the polarizability of montmorillonite molecules may be different; thus, the Hamaker constant will be different subsequently. Usually, the higher the field strength is, the larger the values of the dipole moment and polarizability will be; this will further lead to a higher Hamaker constant. From Figure 5, we can see that at values of the surface potential larger than -267 mV, the values of the Hamaker constant really appear in this relationship. However, at surface potentials lower than 267 mV in absolute value, the results are opposite to the case at surface potentials higher than 267 mV in absolute value. We may expect that it is relevant to the dipole orientation or the direction of the dipole moment vector in the inner structure of the montmorillonite. For example, if more isomorphic substitutions take place in the Si-tetrahedron than in the Al-octahedron for the montmorillonite, the direction of the dipole moment vector will be from the inside to out, the negative surface potential will weaken the dipole moment and the polarizability of the montmorillonite, and the Hamaker constant will decrease with an increase of the surface potential and vice versa. Showing that as the surface potential was lower than 267 mV in absolute value, for the montmorillonite, there might be more isomorphic substitutions taking place in the Si-tetrahedron than in the Al-octahedron. Therefore, if more isomorphic substitutions take place in the Si-tetrahedron, the surface potential for the montmorillonite will be lower than the montmorillonite of more isomorphic substitutions taking place in the Al-octahedron. Under the same conditions, a lower surface potential means a lower value of the charge density on the surface. Therefore, if more isomorphic substitutions take place in the Si-tetrahedron, the surface charge density for the montmorillonite will be lower than that of more isomorphic substitutions taking place in the Al-octahedron. On the other hand, if more isomorphic substitutions take place in the Si-tetrahedron, the atom ratio of Si/Al will be lower than that of more isomorphic substitutions taking place in the Al-octahedron. Therefore, a higher surface charge density must correspond to a higher Si/Al ratio of the montmorillonite. This analysis just meets the well-known fact in soil science that the higher Si/Al ratio will correspond to a higher surface charge density for clays. Therefore, a deduction may be made here that for the montmorillonite with a surface potential lower than 267 mV in absolute value, because more isomorphic substitutions have taken place in the Si-tetrahedron than in the Al-octahedron, the Hamaker constant decreases with increasing surface potential and vice versa.

Considering the surface potential-dependent nature of the Hamaker constant, modification of the classic DLVO theory is needed. On the basis of the classic DLVO theory, the two forces, the electric repulsive force and the van der Waals attractive force, control the behavior of colloidal particles in suspension.

TABLE 5: Effective Hamaker Constants of Montmorillonites with Different Surface Potentials

$\phi(0)$ , mV	$A_{\text{eff}} \times 10^{20}$				$\phi(0)$ , mV	$A_{\text{eff}} \times 10^{20}$			
	7 atm	5 atm	4atm	mean $A_{\text{eff}} \times 10^{20}$		7 atm	5 atm	4atm	mean $A_{\text{eff}} \times 10^{20}$
-255	4.00	6.35	9.11	6.49 ( $\pm 1.69$ )	-275	2.91	3.98	3.31	3.40 ( $\pm 0.377$ )
-259	3.37	5.27	8.22	5.62 ( $\pm 1.73$ )	-277	3.29	4.30	3.52	3.70 ( $\pm 0.396$ )
-263	2.29	3.55	5.91	3.92 ( $\pm 1.33$ )	-278	3.42	4.62	3.54	3.86 ( $\pm 0.401$ )
-264	1.89	3.16	5.14	3.40 ( $\pm 1.16$ )	-279	3.67	4.78	3.75	4.07 ( $\pm 0.476$ )
-265	1.34	2.48	4.14	2.65 ( $\pm 1.00$ )	-280	3.80	4.94	3.77	4.17 ( $\pm 0.513$ )
-266	1.26	1.99	2.87	2.04 ( $\pm 0.553$ )	-281	4.06	5.11	3.98	4.38 ( $\pm 0.482$ )
-267	1.38	2.14	2.11	1.88 ( $\pm 0.331$ )	-283	4.33	5.60	4.21	4.71 ( $\pm 0.589$ )
-268	1.61	2.44	2.30	2.12 ( $\pm 0.337$ )	-284	4.46	5.77	4.23	4.82 ( $\pm 0.631$ )
-269	1.84	2.59	2.49	2.31 ( $\pm 0.309$ )	-286	4.86	6.11	4.47	5.15 ( $\pm 0.644$ )
-270	1.95	2.89	2.50	2.45 ( $\pm 0.331$ )	-287	5.00	6.29	4.49	5.26 ( $\pm 0.689$ )
-271	2.19	3.05	2.69	2.64 ( $\pm 0.304$ )	-291	5.57	6.98	4.99	5.85 ( $\pm 0.755$ )
-272	2.43	3.35	2.89	2.89 ( $\pm 0.306$ )	-295	6.16	7.69	5.29	6.38 ( $\pm 0.868$ )
-273	2.55	3.51	3.09	3.05 ( $\pm 0.332$ )					

Our result shows that not only does the surface potential lead to a repulsive force between two adjacent particles but it also influences the van der Waals attractive force. Therefore, eq 3 would be expressed as

$$P_{\text{vdw}}(\lambda) = \frac{A_{\text{eff}}[\phi(0)]}{0.6\pi} \lambda^{-3} \quad (12)$$

Nevertheless, there are several problems with the determined results of the Hamaker constant at surface potentials lower than 267 mV in absolute value in this study. (1) The experimental data shown in Table 5 indicate that the big relative error exists at surface potentials lower than 267mV in absolute value for different applied pressures; the relative errors often exceed 30% for the effective Hamaker constant. However, for the absolute Hamaker constant in vacuum, the relative error was about 17%. (2) The obtained Hamaker constant seems to be applied pressure dependent, and seemingly with decreasing applied pressure the Hamaker constants increase. However, the Hamaker constant is impossible to be applied pressure dependent. At surface potentials below 267mV in absolute value, the pressure-dependent result for the determined Hamaker constant comes from the systematic error in its calculation. The Hamaker constant calculation was based on the determinations of  $\lambda$  and  $\phi(0)$ , and the experimental errors for  $\lambda$  and  $\phi(0)$  were random errors. However, we used the linear fitting equations based on the experimental data of the relationship between  $\lambda$  and  $\phi(0)$  to calculate both  $P_{\text{vdw}}$  and  $A_{\text{eff}}$ ; therefore, the random error for  $\lambda$  in experiment has been transformed to the systematic error in the  $A_{\text{eff}}$  calculation.

When the surface potentials exceed 267 mV in absolute value, the experimental errors at different applied pressures immediately decrease to 12% on average for the effective Hamaker

constant. However, for the absolute Hamaker constant, the relative error was only 5.8% on average. Therefore, the determined Hamaker constants for surface potentials higher than 267 mV will be more reliable than that for surface potentials lower than 267 mV for the montmorillonites.

The experimental error for the Hamaker constant determination comes from two aspects. One is the experimental error of the distance between two adjacent particles,  $\lambda$ ; another is the experimental error of the van der Waals force,  $P_{\text{vdw}}$ . If the applied pressure is high, the determined  $\lambda$  will be small and the determined  $P_{\text{vdw}}$  will be large. Therefore, the experimental error for  $\lambda$  will be large and for  $P_{\text{vdw}}$  will be small as the applied pressure is high. On the contrary, if the applied pressure is relatively low, the experimental error for  $P_{\text{vdw}}$  will be large and the experimental error for  $\lambda$  will be small accordingly. From eq 3, we can see that the Hamaker constant will be very sensitive to  $\lambda$  since it is directly proportional to  $\lambda^3$ ; a small error in  $\lambda$  will lead to a big error in  $A_{\text{eff}}$ . Therefore, a relatively large value for  $\lambda$  is critical for reducing the relative error in  $A_{\text{eff}}$  determination, which requires a relatively low applied pressure. Therefore, for an applied pressure of 7 atm, the relatively large systematic errors in  $A_{\text{eff}}$  calculation might exist, especially at surface potentials below 267 mV in absolute value. However, as the value of  $\lambda$  is too large, the  $P_{\text{vdw}}$  value will be too low; therefore, the experimental error for  $P_{\text{vdw}}$  will become large as well, which will lead to a large error in  $A_{\text{eff}}$  calculation. Therefore, for applied pressures of 4 atm or less, the relatively large systematic errors in  $A_{\text{eff}}$  calculation might also exist. As the applied pressure was 3 atm, the obtained van der Waals force was so low that it might be less than 0.1 atm. This is the reason why we did not use the experimental data when the applied pressure was 3 atm or less. Showing that as the applied pressures is 5 atm, the experimental error for Hamaker constant determination will be the smallest according to the above analysis. Thus, even though we used the average value in Table 5 to plot the relationship curve between  $A$  and  $\phi(0)$  shown in Figure 5, here we strongly recommend using the determined results of  $A$  as the applied pressure is 5 atm.

#### 4. Conclusions

The van der Waals force and Hamaker constant were determined through the swelling pressure determination of different montmorillonites with different surface potentials in aqueous solution. The results showed that the swelling pressure method could be used in both van der Waals force and Hamaker constant determinations. According to the obtained Hamaker constants for different montmorillonites with differential

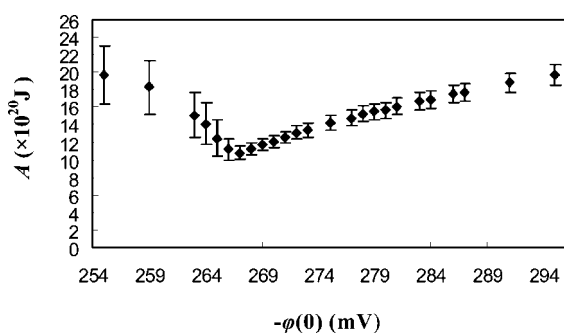


Figure 5. Hamaker constants for different montmorillonites with different surface potentials.

surface potentials, an important feature for the Hamaker constant was observed: the Hamaker constant of montmorillonite was surface potential dependent. At values of the surface potential larger than  $-267$  mV, the values of the Hamaker constant increase with an increase of the surface potential; nevertheless, at surface potentials lower than  $-267$  mV, the Hamaker constant appeared to decrease with an increase of the surface potential. Those phenomena may be relevant to the isomorphic substitution of the montmorillonite. If more isomorphic substitutions take place in the Al-octahedron than that in the Si-tetrahedron for the montmorillonite, the direction of the dipole moment vector will be from out to inside, the negative surface potential will strengthen the dipole moment and the polarizability of the montmorillonite, the Hamaker constant will increase with an increase of the surface potential, and vice versa. Because the surface potential influences both the van der Waals attractive force and the electric repulsive force, modification of the classic DLVO theory may be needed.

**Acknowledgment.** This work was supported by the National Natural Science Foundation of China (Grant Nos. 40671090 and 40740420660).

## References and Notes

- (1) Liang, Y.; Hilal, N.; Langston, P.; Starov, V. *Adv. Colloid Interface Sci.* **2007**, *134–135*, 151–166.
- (2) Pashley, R. M. *J. Colloid Interface Sci.* **1981**, *80*, 153–162.
- (3) Pashley, R. M. *J. Colloid Interface Sci.* **1981**, *83*, 531–546.
- (4) Butt, H. J. *Biophys. J.* **1991**, *60*, 1438–1444.
- (5) Chapel, J. P. *Langmuir* **1994**, *10*, 4237–4243.
- (6) Pashley, R. M.; Israelachvili, J. N. *J. Colloid Interface Sci.* **1984**, *101*, 511–523.
- (7) McGuiggan, P. M.; Pashley, R. M. *J. Colloid Interface Sci.* **1988**, *124*, 560–569.
- (8) Ducker, W. A.; Pashley, R. M. *Langmuir* **1992**, *8*, 109–112.
- (9) Tabor, F. R. S. D.; Winterton, R. H. S. *Proc. R. Soc.* **1969**, *312*, 435.
- (10) Hough, D. B.; White, L. R. *Adv. Colloid Interface Sci.* **1980**, *14*, 3.
- (11) Israelachvili, J. N.; Adams, G. E. *J. Chem. Soc., Faraday Trans.* **1978**, *74*, 975.
- (12) Horn, R. G.; Clarke, D. R.; Clarkson, M. T. *J. Mater. Res.* **1988**, *3*, 413.
- (13) Soma, Das; Sreeram, P. A.; Raychaudhuri, A. K. *Nanotechnology* **2007**, *18*, 035501.
- (14) Butt, H. J.; Cappella, B.; Kappl, M. *Surf. Sci. Rep.* **2005**, *59*, 1.
- (15) Burnham, N. A.; Dominguez, D. D.; Mowery, R. L.; Colton, R. J. *Phys. Rev. Lett.* **1990**, *64*, 1931.
- (16) Ederth, T. *Langmuir* **2001**, *17*, 3329.
- (17) Seog, J.; Dean, D.; Plaas, A. H. K.; Wong-Palms, S.; Grodzinsky, A. J.; Ortiz, C. *Macromolecules* **2002**, *35*, 5601.
- (18) Ackler, H. D.; French, R. H.; Chiang, Y. M. *J. Colloid Interface Sci.* **1996**, *179*, 460.
- (19) Wensink, K. D. F.; Jérôme, B. *Langmuir* **2002**, *18*, 413.
- (20) Håkon, K. *Langmuir* **2006**, *22*, 9234–9237.
- (21) Castellanos, A. J.; Ma'ximo, G.-S.; German, U.-V. *J. Phys. Chem. B* **2003**, *107*, 8532–8537.
- (22) Low, P. F. *Soil Sci. Soc. Am. J.* **1980**, *44*, 667–676.
- (23) Hu, J.; Yang, Z.; Zhen, Z. *Colloid and Interface Science*; South China University of Technology Press: Guang Zhou, 1997 (in Chinese).
- (24) Li, H.; Wei, S.; Qing, C.; Yang, J. *J. Colloid Interface Sci.* **2003**, *258*, 40–44.
- (25) Jie, H.; Li, H.; Wu, L.; Zhu, H. *Soil Sci. Soc. Am. J.* **2009** (accepted).
- (26) Zhang, Z. Z.; Sparks, D. L.; Scrivner, N. C. *J. Colloid Interface Sci.* **1994**, *162*, 244–251.
- (27) Missanal, T.; Adell, A. *J. Colloid Interface Sci.* **2000**, *230*, 150–156.
- (28) Bolt, G. H. *J. Colloid Sci.* **1955**, *10*, 206.

JP808372R